

Representation Synthesis by Probabilistic Many-Valued Logic Operation in Self-Supervised Learning

Hiroki Nakamura¹, Masashi Okada¹,
Tadahiro Taniguchi^{1,2}

¹Panasonic Holdings, Kadoma, Osaka 571-8501 JAPAN

²Ritsumeikan University, Kyoto, Kyoto 604-8520 JAPAN

Corresponding author: Hiroki Nakamura (email: nakamura.hiroki003@jp.panasonic.com)

ABSTRACT Self-supervised learning (SSL) using mixed images has been studied to learn various image representations. Existing methods using mixed images learn a representation by maximizing the similarity between the representation of the mixed image and the synthesized representation of the original images. However, few methods consider the synthesis of representations from the perspective of mathematical logic. In this study, we focused on a synthesis method of representations. We proposed a new SSL with mixed images and a new representation format based on many-valued logic. This format can indicate the feature-possession degree, that is, how much of each image feature is possessed by a representation. This representation format and representation synthesis by logic operation realize that the synthesized representation preserves the remarkable characteristics of the original representations. Our method performed competitively with previous representation synthesis methods for image classification tasks. We also examined the relationship between the feature-possession degree and the number of classes of images in the multilabel image classification dataset to verify that the intended learning was achieved. In addition, we discussed image retrieval, which is an application of our proposed representation format using many-valued logic.

INDEX TERMS logic operation, many-valued logic, representation learning, self-supervised learning

I. INTRODUCTION

Self-supervised learning (SSL) is a method for learning representations without labeled data [1]–[10]. The use of models pre-trained by SSL for image classification and object detection achieves high performance with a small amount of labeled data. Non-contrastive learning, a popular SSL method, e.g., BYOL [2], SimSiam [1], DINO [11], learns a model to maximize the feature similarity of pairs of augmented images. Some SSL methods, such as MixSiam [12], Unmix [13], i-Mix [14] and SDMP [15], have been proposed using a mixture of two images. By adding mixed images as an augmentation method, more image features can be learned, which is effective for various downstream tasks. SDMP [15] learns to make the representation of the mixed image closer to a synthesis of the representation of the pre-mixed image, where the representations of the pre-mixed image are synthesized by a mean operation.

The mean operation is often used to synthesize labels when learning single-label classification using mixed im-

ages [16]–[19]. The maximum operation is also used for learning multilabel classification with mixed images [20]–[23]. The preferred synthesis method differs among tasks because of the different nature of the tasks and labels.

Although label synthesis methods have been proposed based on the characteristics of classification tasks, few methods for synthesizing representations suitable for SSL have been discussed from the perspective of mathematical logic. One reason for this could be it is difficult for humans to understand the features of an image from its SSL representation. It is in contrast to the label of classification, which can indicate the objects present in an image from the values of each dimension of the label. Existing SSL representation synthesis methods [12], [15] follow the label synthesis methods used in classification, such as the mean and maximum operations, although the properties of the classification labels and representations of SSL are different. If the values of each representation dimension can be shown so that humans can understand them, the performance of

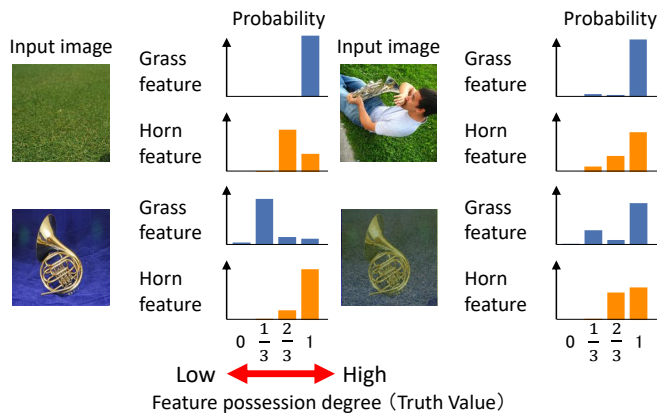


FIGURE 1: Overview of the representation format of our method. The method outputs a representation of how well each image feature is possessed. The representation consists of several categorical distributions. Each categorical distribution corresponds to an image feature, and the probability of the truth value expresses the corresponding feature-possession degree. These examples show two categorical distributions, possibly corresponding to “grass” and “horn.”

downstream tasks may be improved by proposing more suitable representation synthesis methods. Furthermore, there is potential for expanding the applications of representation.

To this end, we propose a new representation format and representation synthesis method. Our new representation format expresses the feature-possession degree by incorporating many-valued logic. The feature-possession degree indicates how much of each image feature a representation possesses. Fig. 1 shows an overview of the representation format. Logic operations as a synthesis method are used to synthesize representations that retain the characteristics of the representations before mixing. The contributions of this study are summarized as follows;

- We proposed a new SSL method using mixed images. This method focused on representation synthesis by incorporating many-valued logic. Our method learns a representation that indicates the degree of image feature possession.
- We conducted experiments on single and multilabel classification tasks and demonstrated that our method is competitive with existing synthetic methods.
- We demonstrated that the synthesized representations successfully express the degree of feature possession without labels. We evaluated the degree of feature possession by examining its relationship with the number of classes in an image.
- Using qualitative results, we demonstrated that image retrieval is a new application of representation synthesized by many-valued logic. Through this method, we achieved image retrieval based on the features of the two images.

II. RELATED WORK

A. Self-supervised learning

Some studies [1]–[3], [5], [11] have shown that SSL performs well in many downstream tasks, such as classification, object detection, and semantic segmentation. SimCLR [5] and MoCo [3], called contrastive learning, learn to maximize the similarity of representation pairs augmented from the same image (*positive pairs*) and to minimize the similarity of representation pairs augmented from different images (*negative pairs*). Meanwhile, SimSiam [1], BYOL [2] and DINO [11], called non-contrastive learning, learn a model using only the positive pairs.

Recently, some studies [13]–[15], [24], [25] have proposed SSL methods with mixed images to learn more diverse image features. Ren et al. [15] proposed SSL based on a transformer using mixed images. Zhang et al. [25] proposed SSL using mixed images from different domains for learning representations of datasets, such as medical image datasets, composed of similar images. MixSiam [25] is an SSL method that uses mixed images and representations synthesized by a maximizing operation to learn more discriminative representations. However, MixSiam uses a mix of two augmentation images obtained from a single image and involves less variation among images than other methods with mixed images. In our method, we discuss the representation synthesis of the SSL.

B. Deep learning with image and label mixtures

Many image mixing methods [16]–[18], [26]–[28] have been proposed for data augmentation method. These methods are mainly applied to train models that are robust to unknown data because they increase the data variation [16]–[22], [29]–[31]. Because a mixed image requires two or more images, it is often impossible to directly use the labels of the original images. Zhang et al. proposed a method for single-label classification [18] that uses an alpha-blended mixture of two images. They used a synthesis of the image labels as the label of the mixed image. Wang et al. proposed a method with mixed images for multilabel classification [20] using an alpha-blended mixture of two images and the labels synthesized by union operation. Alfassy et al. proposed the semi-supervised learning of multilabel classification with two images as the input [23]. This method learns to estimate the union, intersection, and subtraction of the labels of the input images. Thus, the choice of the method for synthesizing labels depends on the target task. However, few methods have been discussed for mixing representations in SSL.

C. Many-valued logic

Many-valued logic is a logic system with vague states, wherein truth values other than the binary values of 0 and 1 can exist. Vague states allow uncertainty expression, and many-valued logic is applied in various tasks in which uncertainty should be considered [32]–[34]. Kumar et al. [32] proposed a more robust image classification incorporating

fuzzy theory into the support vector machine to consider uncertainty. Some methods incorporate many-valued logic into representation learning using deep learning [35]–[37]. Feng et al. [37] proposed a method for auto-encoder-based representation learning in which the variance of features that belong to the same cluster is reduced to learn clustered features easily. Optimization is facilitated by flexible soft clustering based on fuzzy logic instead of hard clustering. However, to the best of our knowledge, no method that uses many-valued logic operations in representation synthesis has been proposed.

III. METHOD

We propose a representation synthesis method based on many-valued logic. The synthesis method produces a representation that holds the features of both representations of the two input images. First, we describe many-valued logic in Sec. III-A. Second, Sec. III-B, we describe the learning of representations with mixed images in a self-supervised manner. Then, we discuss the representation synthesis method in SSL with mixed images in Sec. III-C.

A. Logic operation of many-valued logic

Many-valued logic refers to a logic system with truth values other than 0 and 1. In this study, we considered Gödel logics [38]. In Gödel logics, a family G_k of many-valued logic has k truth values $0, \frac{1}{k-1}, \frac{2}{k-1}, \dots, 1$. The logic operations of variables A and B are defined as follows. A and B are the truth values, and $A, B \in [0, 1]$.

$$A \vee B := \max(A, B) \quad (1)$$

$$A \wedge B := \min(A, B) \quad (2)$$

When A and B follow categorical distribution, they are written as follows.

$$A \sim \text{Cat}(A|\pi_{\mathbf{a}} = \{a_0, a_1, \dots, a_{n-1}\}) \quad (3)$$

$$B \sim \text{Cat}(B|\pi_{\mathbf{b}} = \{b_0, b_1, \dots, b_{n-1}\}) \quad (4)$$

where a_i and b_i represent probabilities. We define $P(A = \frac{i}{n-1}) = a_i$ and $P(B = \frac{i}{n-1}) = b_i$.

Then, we discuss $P(A \vee B = \frac{i}{n-1})$ and $P(A \wedge B = \frac{i}{n-1})$. They are written as;

$$P(A \vee B = \frac{i}{n-1}) = a_i \sum_{j=0}^i b_j + b_i \sum_{j=0}^i a_j - a_i b_i, \quad (5)$$

$$P(A \wedge B = \frac{i}{n-1}) = a_i \sum_{j=i}^{n-1} b_j + b_i \sum_{j=i}^{n-1} a_j - a_i b_i. \quad (6)$$

Fig. 2 shows an example of the probability of each truth value of A, B , and $A \vee B$ for $n = 4$; if the probability of either A or B being larger is high, the probability of $A \vee B$ being larger is also high.

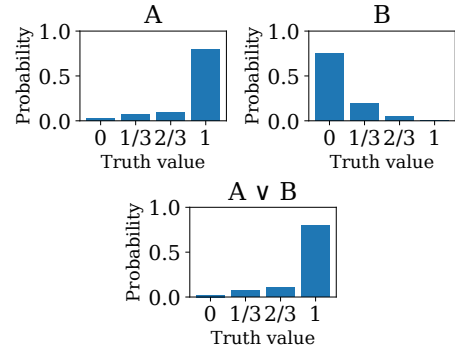


FIGURE 2: Example of the probability of each truth value of A, B , and $A \vee B$ for $n = 4$. If the expected value of the truth value of either one of A or B is large, the expected value of $A \vee B$ is also large.

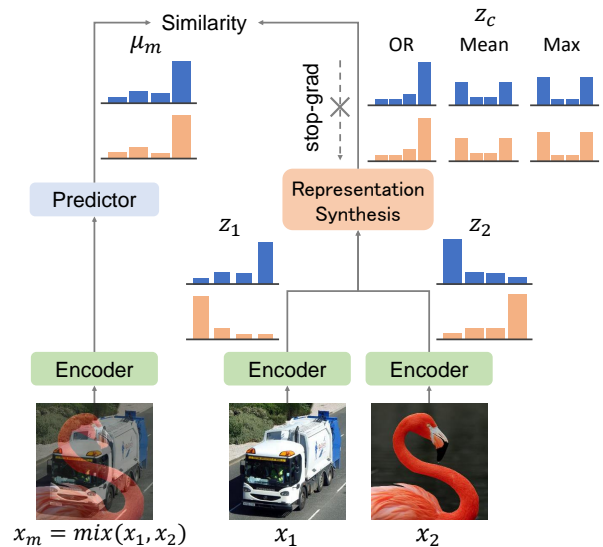


FIGURE 3: Overview of self-supervised learning by mixed images and representation synthesis. This figure shows examples of representation synthesis, such as the logic (OR), mean, and maximum operations.

B. Self-supervised learning with representation synthesis

Our method is based on SimSiam [1], which is a non-contrastive SSL, and incorporates new representation synthesis by many-valued logic. Fig. 3 shows an overview of the SSL method using mixed images and representation synthesis. The method learns representation generation by minimizing the distance of representations of images x_i and x_i' obtained by the random augmentation of an image X_i . Here, i indicates the number of the image. We use encoder f and predictor h to predict representations z_i, z_i' and p_i, p_i' .

$$\tilde{z}_i = f(x_i) \quad (7)$$

$$\tilde{p}_i = h(f(x_i)) \quad (8)$$

$$z_{i,j} = \text{softmax}((\tilde{z}_{i,j} - c)/\tau_t) \quad (9)$$

$$p_{i,j} = \text{softmax}(\tilde{p}_{i,j}/\tau_s) \quad (10)$$

Representations z_i and p_i follow N M -dimensional categorical distribution with the total dimension $N \times M$. Each categorical distribution is defined as $z_{ij}, p_{i,j}$. Thus, $z_{i,j}, p_{i,j} \in \mathbb{R}^M$ and $z_i, p_i \in \mathbb{R}^{N \times M}$. Denote the k -th class parameter of the j -th categorical distribution by $z_{i,j,k}, p_{i,j,k} \in [0, 1]$. τ_t and τ_s are the parameters of sharpening and c is a parameter of centering [11]. By considering cross-entropy, the distance between p and z is written as follows.

$$\mathcal{D}(p_i, z'_i) = -\frac{1}{N} \sum_{j=1}^N \sum_{k=1}^M z'_{i,j,k} \log p_{i,j,k} \quad (11)$$

The loss function is defined as follows. Stop-gradient operation $\text{stopgrad}(\cdot)$ prevents learning collapse.

$$\mathcal{L}_{normal} = \frac{1}{2} \mathcal{D}(p_i, \text{stopgrad}(z'_i)) + \frac{1}{2} \mathcal{D}(p'_i, \text{stopgrad}(z_i)) \quad (12)$$

In addition, our method also learns representation using the mixed image x_{mix} and the synthesized representation z_c . We use Mixup [18] to generate mixed image x_{mix} , and we generate z_c using representations z_1 and z_2 and synthesis function $\text{Mix}(\cdot)$.

$$x_{mix} = \lambda_{mix} x_1 + (1 - \lambda_{mix}) x_2, \quad (13)$$

$$z_c = \text{Mix}(z_1, z_2) \quad (14)$$

We define another loss function \mathcal{L}_{mix} to minimize the distance between p_{mix} , which is the representation of x_{mix} and the synthesized representation z_c . We also define the weighted average of \mathcal{L}_{normal} and \mathcal{L}_{mix} as the final loss function \mathcal{L} .

$$\mathcal{L}_{mix} = \mathcal{D}(p_{mix}, \text{stopgrad}(z_c)), \quad (15)$$

$$\mathcal{L} = \alpha \mathcal{L}_{normal} + (1 - \alpha) \mathcal{L}_{mix} \quad (16)$$

C. Representation synthesis

In this section, we explain the representation synthesis methods. First, we describe the synthesis of representations by mean and maximum operations used in existing methods. Then, we describe representation synthesis by many-valued logic operation.

Representation synthesis by mean operation

This synthetic method is referenced from SDMP [15]. The synthesized representation z_c is derived from z_1, z_2 , and Mixup parameter λ_{mix} .

$$z_c = \lambda_{mix} z_1 + (1 - \lambda_{mix}) z_2 \quad (17)$$

Representation Synthesis by Maximum Operation

This synthetic method is referenced from MixSiam [12]. The synthesized representation z_c is the normalized element-wise maximum of the prenormalized representations $f(x_1)$ and $f(x_2)$. maximum means the element-wise maximum function, and z_c is derived as follows;

$$z_{c,j} = \text{softmax} \left(\frac{\text{maximum}(\tilde{z}_{1,j}, \tilde{z}_{2,j}) - c}{\tau_t} \right). \quad (18)$$

Representation synthesis by logic operation

We propose a representation synthesis method based on many-valued logic. $Z_{i,j}$ is a stochastic variable that follows the j -th categorical distribution of z_i . When $Z_{i,j}$ follows Gödel logics and has M truth values $(0, \frac{1}{M-1}, \dots, 1)$, $Z_{i,j}$ is written as shown below;

$$Z_{i,j} \sim \text{Cat}(Z_{i,j} | \pi = \{z_{i,j,1}, z_{i,j,2}, \dots, z_{i,j,M}\}), \quad (19)$$

$$P(Z_{i,j} = \frac{k-1}{M-1}) = z_{i,j,k}. \quad (20)$$

In our method, we assume that each categorical distribution corresponds to a feature of an image and that the larger the expected value of $Z_{i,j}$, the more features of the image corresponding to $Z_{i,j}$ that it holds. We designed the synthesis method so that the feature-possession degree, the expected value of $Z_{i,j}$, does not decrease after representation synthesis, i.e., $Z_{c,j} \geq Z_{i,j}$ is satisfied.

We define the representation synthesis of $Z_{1,j}$ and $Z_{2,j}$, using the OR operation of many-valued logic, as discussed in Sec. III-A.

$$Z_{c,j} := Z_{1,j} \vee Z_{2,j} \quad (21)$$

$Z_{c,j}$ is the stochastic variable that follows a categorical distribution after the synthesis of $Z_{1,j}$ and $Z_{2,j}$. $Z_{c,j} \geq Z_{1,j}$ and $Z_{c,j} \geq Z_{2,j}$ are satisfied when the synthesis is performed as in Eq. (21). Each element of the synthetic feature z_c of z_1 and z_2 is derived as follows using Eq. (5).

$$z_{c,j,K} = P(Z_{1,j} \vee Z_{2,j} = \frac{K-1}{M-1}) \quad (22)$$

$$= z_{1,j,K} \sum_{k=1}^K z_{2,j,k} + z_{2,j,K} \sum_{k=1}^K z_{1,j,k} - z_{1,j,K} z_{2,j,K} \quad (23)$$

D. Expected value loss

Our proposed method associates many-valued logic with representations. This section describes a new loss that considers this property. As shown in Eq. (11), the distance between two representations is calculated by cross-entropy, which treats each representation element equally. For example, when there are three stochastic variables of the truth value,

$$Z_{1,j} \sim \text{Cat}(z_{1,j,1} = 0.8, z_{1,j,2} = 0.1, z_{1,j,3} = 0.1),$$

$$Z_{2,j} \sim \text{Cat}(z_{2,j,1} = 0.1, z_{2,j,2} = 0.8, z_{2,j,3} = 0.1),$$

$$Z_{3,j} \sim \text{Cat}(z_{3,j,1} = 0.1, z_{3,j,2} = 0.1, z_{3,j,3} = 0.8)$$

following Eq. (19) and (20), the cross-entropy loss of $Z_{1,j}$ and $Z_{2,j}$ is the same as that of $Z_{1,j}$ and $Z_{3,j}$, though the expected truth values of $Z_{2,j}$ and $Z_{3,j}$ are different. To consider the truth value, we propose the following loss using the expected value of the stochastic variable. Here, $E[\cdot]$

indicates the expected value.

$$\begin{aligned} \text{BCE}(E[Z_{1,j}], E[Z_{2,j}]) = \\ -E[Z_{1,j}] \log E[Z_{2,j}] - (1 - E[Z_{1,j}]) \log (1 - E[Z_{2,j}]) \end{aligned} \quad (24)$$

$$\mathcal{L}_{exp} = \sum_{j=1}^M \text{BCE}(E[Z_{1,j}], E[Z_{2,j}]) \quad (25)$$

Finally, we use the weighted average of \mathcal{L} and \mathcal{L}_{exp} as the loss function.

$$\mathcal{L}_{prop} = \beta \mathcal{L}_{exp} + (1 - \beta) \mathcal{L} \quad (26)$$

IV. EXPERIMENT

In this section, we experiment with the proposed method from several perspectives. First, we verified the proposed representation synthesis method by comparing its performance with that of existing methods for classification tasks (Sec. IV-B, C). As expected, we found that the degree of image feature possession was learned. We validated this degree by examining its relationship to the number of image classes (Sec. IV-D). In addition, we examined the correspondence between the feature-possession degree and objects in the image (Sec. IV-E). We also discussed a new type of image retrieval method that uses synthesized representations (Sec. IV-F).

A. Implementation

Experimental settings for networks The projector of the encoder f and predictor h of the proposed method are the same as those of SimSiam. The backbone network of the encoder f is Resnet-18 [39]. Unless otherwise noted, the number of dimensions of the representation is 4096, the number of categorical distributions within the representations N is 256, and the number of classes in each categorical distribution M is 16.

Experimental settings for pretraining; We used momentum-SGD for pretraining. The learning rate was 0.02, and SGD momentum was 0.9. The learning rate followed a cosine-decay schedule. The weight decay was $1e-4$. The batch size was 32. The parameters of sharpening were $\tau_s = 0.1$ and $\tau_t = 0.04$. The parameter of centering c was updated as in DINO, with the update parameter set to $m = 0.9$. The augmentation settings were the same as those used in SimSiam. The image-mixing method used was Mixup [18]. The parameter for Mixup, λ_{mix} , was set to 0.5 when the synthesis method was the maximum or logic operation. When the synthesis method was the mean operation, λ_{mix} follows a uniform distribution $[0, 1]$. The loss weight α in Eq. (16) is 0.5 and β in Eq. (26) is 0.75.

B. Single-label image classification

We experimented with single-label image classification to verify the effectiveness of our method. First, we performed

TABLE 1: Top-1 accuracy of linear-evaluation For each method, eight experiments are performed, and the mean and standard deviation of the Top-1 accuracy is calculated. The results are expressed as the mean \pm standard deviation.

method	ImageNet100	Cifar10
vanilla	71.12 \pm 0.34	88.98 \pm 0.27
Mean operation [15]	74.35 \pm 0.49	90.75 \pm 0.24
Maximum operation [12]	71.50 \pm 0.56	90.16 \pm 0.38
Logic operation (Ours)	75.46 \pm 0.52	90.18 \pm 0.26

self-supervised pretraining with ImageNet100 [40]¹ and CIFAR10 [41] dataset without labels to learn image representations. Then, we trained a linear classifier on frozen representations on the training set of the dataset with the labels. Finally, we calculated the top-1 accuracy of the test set and used it as an evaluation metric.

Now, we describe the experimental setup for learning a linear classifier. We used LARS [42] as an optimizer for linear evaluation. The learning rate was 1.6, and the SGD momentum was 0.9. The weight decay was 0.0, and the batch size was 512. The image augmentation was performed as done in SimSiam. The number of epochs is 200. We used the model with the highest top-1 accuracy for the validation set for testing. When we trained it, we cropped an image randomly and resized it to 224×224 before inputting it into the model. The area of a random cropped image was from 0.08 to 1.0 of the area of the original image. In the validation and test phase, the image was resized to 256×256 , and the center was cropped to 224×224 .

Tab. 1 summarized the results. We compared four methods: vanilla (not using mixed images) and representation synthesis by mean, maximum, and logic operations. Our method performs competitively with the existing synthetic methods. In particular, our method outperformed other methods with ImageNet100.

C. Multilabel image classification

We also experimented with multilabel image classification to verify the effectiveness of our method. The model pre-trained at 200 epochs by ImageNet100 was trained on the multilabel classification dataset and evaluated in terms of the mean-average-precision (mAP).

Experiments were performed under two conditions: one in which the backbone network was fixed and only the final fully-connected layer was trained, and the other in which all layers were trained. When only the final fully-connected layer was trained, the number of epochs was 500, and the learning rate was 0.02. When all layers were trained, the number of epochs was 200, and the learning rate was $1e-4$. The learning rate was divided by 10 when the error plateaued. When we trained the models, the input image was resized to 640×640 , and we randomly selected $\{640, 576,$

¹ImageNet100 is a 100-category subset of ImageNet [40].

TABLE 2: Results of multilabel classification For each method, eight experiments are performed, and the mean and standard deviation of mAP are calculated. The results are expressed as the mean \pm standard deviation.

method	Pascal VOC	COCO
freeze backbone network		
vanilla	61.10 \pm 0.32	43.43 \pm 0.17
Mean operation [15]	61.76 \pm 0.43	43.95 \pm 0.20
Maximum operation [12]	60.17 \pm 0.38	42.59 \pm 0.29
Logic operation (Ours)	62.49 \pm 0.58	44.89 \pm 0.52
finetuning		
vanilla	67.49 \pm 0.65	64.20 \pm 0.18
Mean operation [15]	68.14 \pm 0.94	64.95 \pm 0.30
Maximum operation [12]	68.22 \pm 0.51	64.59 \pm 0.12
Logic operation (Ours)	68.58 \pm 0.91	65.24 \pm 0.30

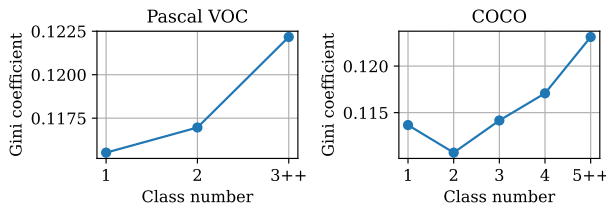


FIGURE 4: Relationship between the image feature-possession degree and the number of image classes.

512, 384, 320} as the width and height to crop the images. Finally, the cropped images were resized to 224 \times 224 pixels. When we evaluated the models, we resized the input image to 256 \times 256 and performed center-crop operation with a size of 224 \times 224.

We used Microsoft COCO [43] and Pascal VOC [44] as multilabel classification datasets, which contain 80 and contains 20 categories, respectively. When using COCO, we trained models using the training set and evaluated them using the validation set because ground truth annotations for the test set were unavailable. When using Pascal VOC, we trained models using the train2007 and train2012 sets and evaluated them using the test2007 set.

Table. 2 shows the results. Our method outperformed other representation synthesis methods.

D. Relationship between image feature-possession degree and the number of image classes

We considered that if many objects are in an image, many feature-possession degrees will be higher. To verify this assumption, we compared the feature-possession degree with the number of classes in the images. We used the Gini coefficient of feature-possession degrees as an indicator. This indicator is often used to measure income disparity. The value is obtained by obtaining the Lorenz curve of the feature-possession degrees in the representation and dividing the area between the line of equality and the Lorenz curve

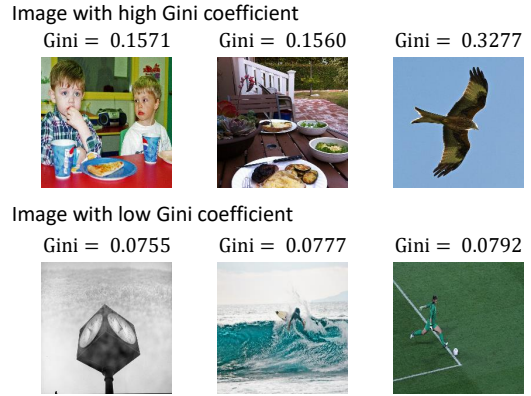


FIGURE 5: Examples of images with the Gini coefficient. Images with a high Gini coefficient tend to show many objects. In contrast, Images with a low Gini coefficient show few objects. However, images with objects clearly visible on a plain background, such as the top right image, tend to have large differences between feature-possession degrees with small and large values, and the Gini coefficient tends to be large despite the small number of objects.

by the area under the line of equality. It is written as follows;

$$Gini = \frac{S - \int_0^1 L(x)dx}{S} \tag{27}$$

$L(x)$ is the Lorenz curve, and x is the cumulative share of the feature-possession degrees from the lowest to highest. The variable S is the area under the line of equality, and $S = 0.5$.

For example, this value is larger when many feature-possession degrees are high and smaller when many feature-possession degrees are not high.

We assumed that the number of features was related to the number of classes of images in Pascal VOC and COCO datasets. Fig. 4 shows the average Gini coefficient for each number of classes. When linear regression was performed on the Gini coefficient and number of classes, the coefficient was significantly positive ($p < 0.01$)². We also show examples of images with high and low Gini coefficients in Fig. 5. These results show that the proposed method makes it possible to represent many features in an image by the feature-possession degree.

E. Relationship between the image feature-possession degree and blur

We examined the effect of augmentation on the image feature-possession degree. We used Gaussian blur for augmentation. First, we observed changes in the distribution of the feature-possession degrees after applying Gaussian blur to the images. The distribution of the feature-possession degrees for the validation set of ImageNet100 is shown in Fig. 6. A comparison of the distributions with and without blurring shows that the variance of the feature-possession

²How to calculate the p-value is mentioned in Appx. A.

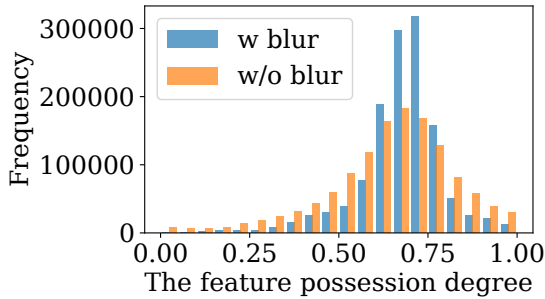


FIGURE 6: Comparison of the distributions of the feature-possession degrees with and without Gaussian blurring on the image. Blurring makes it difficult to recognize whether a feature is present or not. Thus, it is less likely that the feature-possession degrees can be predicted to be extremely high or low.

degree is smaller when blurring is applied. It can be assumed that blurring reduces the confidence level of the existence or absence of certain features, making it less likely to be predicted as having an extremely high or low feature-possession degree.

Next, we discuss the relationship between some regions of the image and the feature-possession degrees. Fig. 7 shows the probability distribution Z of the truth values of the feature-possession degree in the original and blurred images. The images in the top row represent the original images. Both Z_{13} and Z_{18} have high feature-possession degrees. The images in the second row are blurred, indicating uncertainty in both degrees of feature possession. The third and fourth rows show the cases in which only a portion of the image is blurred. In the left image, the feature-possession degree of Z_{13} does not decrease significantly when the blur is applied to the fish part, but decreases when the blur is applied to other parts of the image. In contrast, in the right image, the feature-possession degree of Z_{18} decreases when the blur is applied to the snail part, and it does not decrease significantly when the blur is applied to other parts of the image. This indicates that Z_{18} corresponds to a snail, but Z_{13} does not correspond to a fish. Thus, the feature-possession degrees correspond to each region of the image.

F. Image retrieval from synthesized representations

Here, we discuss a new type of image retrieval that is realized by expressing the feature-possession degree using the truth value. In our method, the representation is composed of the probability of the truth values of each feature-possession degree. In addition, the truth values can be calculated by OR and AND operations, as mentioned in Sec. III-A. By applying the OR operation to the predicted representations, we can generate representations that possess the features possessed by at least one of the respective representations. By applying the AND operations to the predicted representations, we can generate representations that possess the features commonly possessed by both representations.

TABLE 3: Impact of the number of truth values on performance. ImageNet100 used Top-1 accuracy, and PascalVOC and COCO used mAP as the evaluation metrics.

Class	Dimension	ImageNet100	PascalVOC	COCO
2	512	61.07±9.80	49.78±4.92	35.92±3.67
2	4096	74.17±1.33	61.94±0.44	44.44±0.33
4	4096	33.28±21.50	29.41±14.48	24.72±12.50
8	4096	64.07±9.29	62.00±7.73	29.21±4.75
16	4096	75.46±0.52	62.49±0.58	44.89±0.52
32	4096	73.99±0.46	62.44±0.49	44.68±0.29

Fig. 8 shows examples of images with representations most similar to the representation, synthesizing the representation of the two input images. The dataset was the test set of PascalVOC. The similarity was measured using the sign inversion of Eq. (11). The top row shows an example of the OR operation. The input image A in the top row shows a dog and bedding. The input image B in the top row shows a person and a dark background. Images with similar representations have features of both images, such as images of animals and humans, or those with dark background colors. The bottom row shows an example of the AND operation. The input image A in the bottom row shows a dog and a human. The input image B in the bottom row shows the head of the dog. The images with similar representations mostly show the head of the dog, which are images with features common to both images.

V. ABLATION STUDY

A. Impact of the number of truth values

The representation of this method consists of several categorical distributions, each class of the categorical distribution corresponding to a truth value of many-valued logic. We evaluated our method on ImageNet100, PascalVOC, and COCO datasets, varying the number of truth values of the many-valued logic. Table. 3 shows the results. Here, “Class” indicates the number of a class of a categorical distribution, and “Dimension” represents the total number of dimensions of the representations. ImageNet100 uses top-1 accuracy, and Pascal VOC and COCO use mAP as evaluation metrics. When Class is 2, the expected-value loss in Sec. III-D was not used because it is not considered valid for Class 3 or higher. This result shows that Class 16, which is a many-valued logic, yields the best performance.

B. Impact of the expected value loss

We observed changes in the results with changes in the parameter β in Eq. (26). Tab. 4 shows the top-1 accuracy for ImageNet100. The highest accuracy was achieved at $\beta = 0.75$.

VI. LIMITATION

The computational cost of our representation synthesis method is higher than that of the mean and maximum oper-

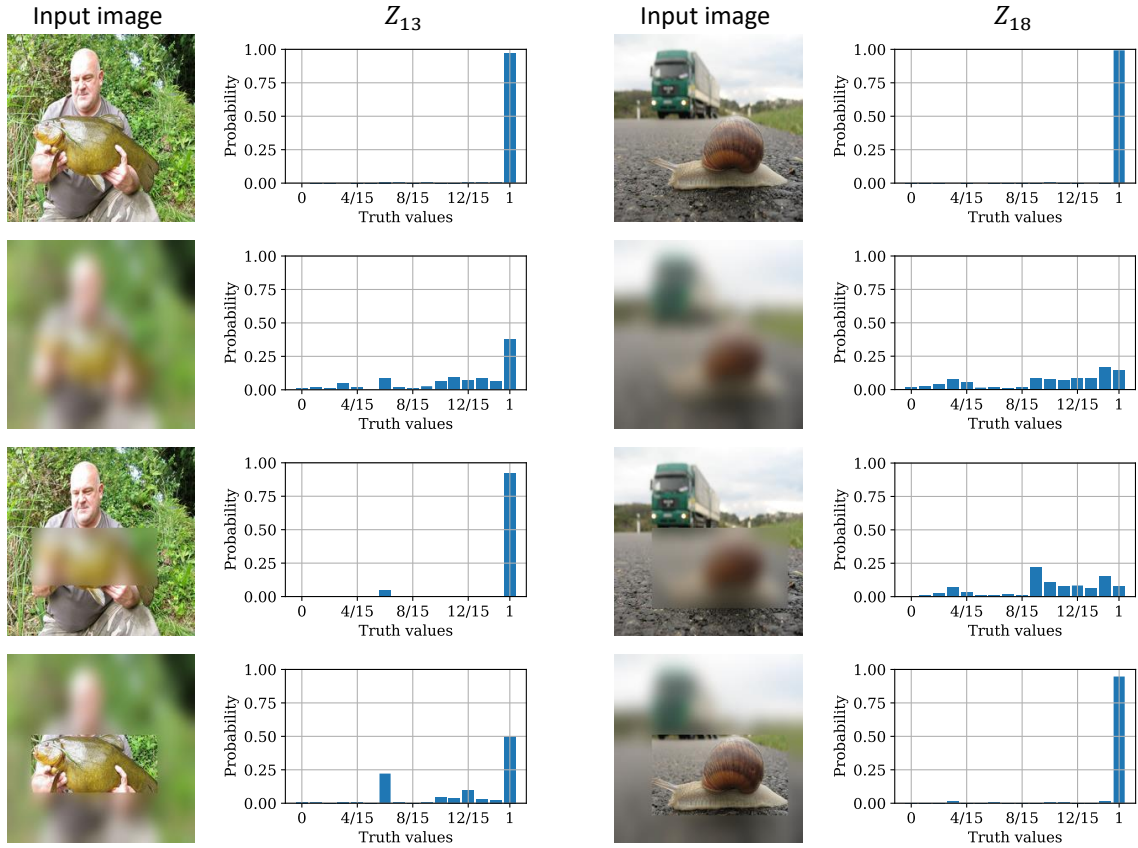


FIGURE 7: Probability distribution of the truth values of the feature-possession degree in the original and blurred images. From the locations where the blur is applied and the change in the distribution of the truth values of Z_i , the corresponding locations in Z_i can be estimated.

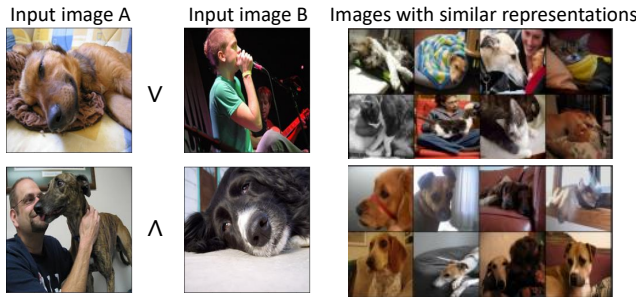


FIGURE 8: Examples of image retrieval from synthesized representations. The examples of images with a representation similar to the OR operation of representations of two images are shown at the top. These images have features of both images. For example, they show both an animal and a human. The examples of images with a representation similar to the AND operation of representations of two images are shown at the bottom. These images have features common to both images. For example, most of them show the heads of dogs.

ation. With existing representation synthesis methods, such as mean and maximum operations, the computational cost is $O(N)$, where N is the number of representation dimensions. In the proposed method, when the number of truth values of

TABLE 4: Impact of the expected value loss on performance. It shows the Top-1 accuracy of ImageNet100 of parameter β in Eq. (26).

β	0.0	0.25	0.5	0.75	0.9
	72.98 ± 0.43	72.83 ± 0.61	73.48 ± 0.38	75.46 ± 0.52	2.38 ± 1.69

the categorical distribution Z_i in the representation is M , the cost is $O(M^2)$.

VII. CONCLUSION

In this study, we focused on a representation synthesis method for SSL and proposed SSL based on a new representation format by incorporating many-valued logic and the representation synthesis method by logic operation. We experimentally demonstrated that the performance of our method is competitive with that of the existing representation synthesis methods in some image classification tasks. In addition, the proposed representation format expresses the possession degrees of various image features using many-valued logic. We verified the validity of the method by investigating its relationship with the number of classes in multilabel classification tasks. We also discussed the applications of the proposed method, such as image retrieval using synthesized representations.

REFERENCES

- [1] Xinlei Chen and Kaiming He, “Exploring simple siamese representation learning,” in *CVPR*, 2021.
- [2] Jean-Bastien Grill, Florian Strub, Florent Altché, Corentin Tallec, Pierre Richemond, Elena Buchatskaya, Carl Doersch, Bernardo Avila Pires, Zhaohan Guo, Mohammad Gheshlaghi Azar, et al., “Bootstrap your own latent—a new approach to self-supervised learning,” *NeurIPS*, 2020.
- [3] Kaiming He, Haoqi Fan, Yuxin Wu, Saining Xie, and Ross Girshick, “Momentum contrast for unsupervised visual representation learning,” in *CVPR*, 2020.
- [4] Xinlei Chen, Saining Xie, and Kaiming He, “An empirical study of training self-supervised vision transformers,” in *ICCV*, 2021.
- [5] Ting Chen, Simon Kornblith, Mohammad Norouzi, and Geoffrey Hinton, “A simple framework for contrastive learning of visual representations,” in *International conference on machine learning*. PMLR, 2020, pp. 1597–1607.
- [6] Jure Zbontar, Li Jing, Ishan Misra, Yann LeCun, and Stéphane Deny, “Barlow twins: Self-supervised learning via redundancy reduction,” in *ICML*, 2021.
- [7] Yuandong Tian, Xinlei Chen, and Surya Ganguli, “Understanding self-supervised learning dynamics without contrastive pairs,” in *ICML*, 2021.
- [8] Alejandro Newell and Jia Deng, “How useful is self-supervised pretraining for visual tasks?,” in *CVPR*, 2020.
- [9] Nikos Komodakis and Spyros Gidaris, “Unsupervised representation learning by predicting image rotations,” in *ICLR*, 2018.
- [10] Mehdi Noroozi and Paolo Favaro, “Unsupervised learning of visual representations by solving jigsaw puzzles,” in *ECCV*, 2016.
- [11] Mathilde Caron, Hugo Touvron, Ishan Misra, Hervé Jégou, Julien Mairal, Piotr Bojanowski, and Armand Joulin, “Emerging properties in self-supervised vision transformers,” in *ICCV*, 2021.
- [12] Xiaoyang Guo, Tianhao Zhao, Yutian Lin, and Bo Du, “Mixsiam: A mixture-based approach to self-supervised representation learning,” *arXiv preprint arXiv:2111.02679*, 2021.
- [13] Zhiqiang Shen, Zechun Liu, Zhuang Liu, Marios Savvides, Trevor Darrell, and Eric Xing, “Un-mix: Rethinking image mixtures for unsupervised visual representation learning,” in *AAAI*, 2022.
- [14] Kibok Lee, Yian Zhu, Kihyuk Sohn, Chun-Liang Li, Jinwoo Shin, and Honglak Lee, “i-mix: A domain-agnostic strategy for contrastive representation learning,” in *ICLR*, 2021.
- [15] Sucheng Ren, Huiyu Wang, Zhengqi Gao, Shengfeng He, Alan Yuille, Yuyin Zhou, and Cihang Xie, “A simple data mixing prior for improving self-supervised learning,” in *CVPR*, 2022.
- [16] Sangdoon Yun, Dongyoon Han, Seong Joon Oh, Sanghyuk Chun, Junsuk Choe, and Youngjoon Yoo, “Cutmix: Regularization strategy to train strong classifiers with localizable features,” in *ICCV*, 2019.
- [17] Kyungjune Baek, Duhyeon Bang, and Hyunjung Shim, “Gridmix: Strong regularization through local context mapping,” *Pattern Recognition*, 2021.
- [18] Hongyi Zhang, Moustapha Cisse, Yann N. Dauphin, and David Lopez-Paz, “mixup: Beyond empirical risk minimization,” in *ICLR*, 2018.
- [19] Jin-Ha Lee, Muhammad Zaigham Zaheer, Marcella Astrid, and Seung-Ik Lee, “Smoothmix: A simple yet effective data augmentation to train robust classifiers,” in *CVPRW*, 2020.
- [20] Qian Wang, Ning Jia, and Toby P. Breckon, “A baseline for multi-label image classification using an ensemble of deep convolutional neural networks,” in *ICIP*, 2019.
- [21] Huiyuan Yang, Taoyue Wang, and Lijun Yin, “Set operation aided network for action units detection,” in *International Conference on Automatic Face and Gesture Recognition*, 2020.
- [22] Jixiang Gao, Jingjing Chen, Huazhu Fu, and Yu-Gang Jiang, “Dynamic mixup for multi-label long-tailed food ingredient recognition,” *IEEE Transactions on Multimedia*, 2022.
- [23] Amit Alfassy, Leonid Karlinsky, Amit Aides, Joseph Shtok, Sivan Harary, Rogerio Feris, Raja Giryes, and Alex M Bronstein, “Laso: Label-set operations networks for multi-label few-shot learning,” in *CVPR*, 2019.
- [24] Sungnyun Kim, Gihun Lee, Sangmin Bae, and Se-Young Yun, “Mixco: Mix-up contrastive learning for visual representation,” *NeurIPS Workshop*, 2020.
- [25] Yichen Zhang, Yifang Yin, Ying Zhang, and Roger Zimmermann, “Mix-up self-supervised learning for contrast-agnostic applications,” in *ICME*, 2022.
- [26] Paola Cascante-Bonilla, Arshdeep Sekhon, Yanjun Qi, and Vicente Ordonez, “Evolving image compositions for feature representation learning,” in *BMVC*, 2021.
- [27] AFM Uddin, Mst Monira, Wheemyung Shin, TaeChoong Chung, Sung-Ho Bae, et al., “Saliencymix: A saliency guided data augmentation strategy for better regularization,” *arXiv*, 2020.
- [28] Zicheng Liu, Siyuan Li, Di Wu, Zihan Liu, Zhiyuan Chen, Lirong Wu, and Stan Z Li, “Automix: Unveiling the power of mixup for stronger classifiers,” in *ECCV*, 2022.
- [29] Zhi Zhang, Tong He, Hang Zhang, Zhongyue Zhang, Junyuan Xie, and Mu Li, “Bag of freebies for training object detection neural networks,” *arXiv*, 2019.
- [30] Yu-Ting Chang, Qiaosong Wang, Wei-Chih Hung, Robinson Piramuthu, Yi-Hsuan Tsai, and Ming-Hsuan Yang, “Mixup-cam: Weakly-supervised semantic segmentation via uncertainty regularization,” *BMVC*, 2020.
- [31] Minghao Xu, Jian Zhang, Bingbing Ni, Teng Li, Chengjie Wang, Qi Tian, and Wenjun Zhang, “Adversarial domain adaptation with domain mixup,” in *AAAI*, 2020.
- [32] Abhinav Kumar, Sanjay Kumar Singh, Sonal Saxena, Amit Kumar Singh, Sameer Shrivastava, K Lakshmanan, Neeraj Kumar, and Raj Kumar Singh, “Comhisp: A novel feature extractor for histopathological image classification based on fuzzy svm with within-class relative density,” *IEEE Transactions on Fuzzy Systems*, 2020.
- [33] Marcin Korytkowski, Leszek Rutkowski, and Rafal Scherer, “Fast image classification by boosting fuzzy classifiers,” *Information Sciences*, 2016.
- [34] Chun-Fu Lin and Sheng-De Wang, “Fuzzy support vector machines,” *IEEE transactions on neural networks*, 2002.
- [35] Dayu Tan, Zheng Huang, Xin Peng, Weimin Zhong, and Vladimir Mahalec, “Deep adaptive fuzzy clustering for evolutionary unsupervised representation learning,” *IEEE Transactions on Neural Networks and Learning Systems*, 2023.
- [36] Yun Wang, Zhenbo Li, Fei Li, Pu Yang, and Jun Yue, “Towards fusing fuzzy discriminative projection and representation learning for image classification,” *Engineering Applications of Artificial Intelligence*, 2022.
- [37] Qiyang Feng, Long Chen, CL Philip Chen, and Li Guo, “Deep fuzzy clustering—a representation learning approach,” *IEEE Transactions on Fuzzy Systems*, 2020.
- [38] Kurt Godel, “Zum intuitionistischen aussagenkalkul,” *Anzeiger Akademie der Wissenschaften Wien, mathematisch-naturwissenschaftliche Klasse*, 1932.
- [39] Kaiming He, Xiangyu Zhang, Shaoqing Ren, and Jian Sun, “Deep residual learning for image recognition,” in *CVPR*, 2016.
- [40] Jia Deng, Wei Dong, Richard Socher, Li-Jia Li, Kai Li, and Li Fei-Fei, “Imagenet: A large-scale hierarchical image database,” in *CVPR*, 2009.
- [41] Alex Krizhevsky, Geoffrey Hinton, et al., “Learning multiple layers of features from tiny images,” 2009.
- [42] Yang You, Igor Gitman, and Boris Ginsburg, “Large batch training of convolutional networks,” *arXiv preprint arXiv:1708.03888*, 2017.
- [43] Tsung-Yi Lin, Michael Maire, Serge Belongie, James Hays, Pietro Perona, Deva Ramanan, Piotr Dollár, and C Lawrence Zitnick, “Microsoft coco: Common objects in context,” in *ECCV*, 2014.
- [44] Mark Everingham, Luc Van Gool, Christopher KI Williams, John Winn, and Andrew Zisserman, “The pascal visual object classes (voc) challenge,” *IJCV*, 2010.

Appendix

A. Test of the relationship between two variables

This section describes whether a variable x is related to a variable y by testing the score a . Scores are assumed to be a relationship between two variables, e.g., coefficients from linear or logistic regression, and AUROC scores, among others.

First, a score is obtained from $X = \{x_1, x_2, \dots, x_N\}$ and $Y = \{y_1, y_2, \dots, y_N\}$. We then set the null hypothesis to H_0 and the alternative hypothesis to H_1 . Set H_0 to mean that X and Y are unrelated and H_1 to mean that they are related. For example, if you want to test whether there is a positive proportion, set $H_0 : a \leq 0$, $H_1 : a > 0$. Then, $Y'_j = \{y'_{j,1}, y'_{j,2}, \dots, y'_{j,N}\}$ is obtained by random shuffling Y . This process creates a set of M dummy objective variables Y'_1, Y'_2, \dots, Y'_M . M dummy scores a'_1, a'_2, \dots, a'_M are obtained from each Y'_j and X . We decide whether to reject H_0 or not by regarding M dummy scores as a test statistic.